Evaluation of Time-Dependent Wall Shear Stress Visualizations for Cerebral Aneurysms

Sylvia Glaßer[1], Jan Hirsch[1], Philipp Berg[2], Patrick Saalfeld[1], Oliver Beuing[3], Gabor Janiga[2], Bernhard Preim[1]

[1] Department of Simulation and Graphics, Otto-von-Guericke University, Magdeburg
[2] Department of Fluid Dynamics and Technical Flows, Otto-von-Guericke-University Magdeburg
[3] Institute of Neuroradiology, Otto-von-Guericke University, Magdeburg

Abstract. For the rupture risk assessment of cerebral aneurysms, the blood flow is approximated using computational fluid dynamics (CFD). Unsteady CFD inflow conditions yield time-dependent vector fields, from which the wall shear stress (WSS), an important indicator for rupture risk in clinical research, is extracted. For WSS evaluation, its magnitude is usually color-coded on the aneurysm surface mesh. Hence, time-dependent results would require an animated depiction of all WSS values. Instead, mostly a static 3D representation is employed by choosing a single point in time, e.g., peak-systole. Our developed framework comprises such a static WSS visualization, an animated visualization, as well as a new technique including statistic information. We compare them in a user study and match them against a ground truth extracted by a clinical expert. The new technique with statistical information turned out to be superior compared to the ground truth for the depiction of time-dependent WSS.

1 Introduction

Cerebral aneurysms are mainly saccular dilatations of cerebral arteries. Aneurysms may rupture frequently leading to death or permanent disability. To prevent rupture of incidentally detected aneurysms, treatment is recommended based on several morphological criteria. These criteria only insufficiently describe the individual rupture risk, yielding a complication rate similar to the estimated annual rupture risk in many cases. Consequently, a better understanding of factors leading to rupture is desired and the rupture risk assessment is an active clinical research area. Complex and irregular blood flow is associated with increased rupture risk [1]. The blood flow is measured (e.g., with Time-of-Flight MRI) or approximated using computational fluid dynamics (CFD) with certain limitations. For instance, the blood is often assumed to be a Newtonian fluid and the vessel wall is modeled as a rigid boundary with infinite resistance. Furthermore, steady CFD simulations with cycle-averaged constant inflow conditions are carried out at the expense of a lower degree of realism. In contrast, for unsteady simulations with a high computational effort, a time-dependent approximation of the blood inflow modeling the cardiac cycle is employed. Steady or unsteady CFD inflow conditions yield constant and time-dependent vector fields, respectively. The CFD evaluation often involves the analysis of wall shear stress (WSS) [2], i.e., the friction of the blood at the aneurysm wall. In clinical research, further parameters are employed, e.g., the oscillating shear index, which is derived from time-dependent WSS and describes how strong this parameter is varying in different directions over time.

In this work, we focus on WSS assessment, which is usually carried out by color-coding of the aneurysm surface. To reduce the temporal information and thus the mental effort to analyze unsteady simulation results, the point in time of the peak systole (where the blood flow is assumed to be at maximum) is chosen in most cases. Since there exist strong differences between the extracted WSS extrema values for steady and unsteady simulations [3], as well as between diastolic and systolic time stages [4], we carried out a user study to assess whether the peak-systolic evaluation is sufficient. Therefore, three techniques were compared: peak-systolic WSS visualization, animated WSS visualization and a new WSS visualization including statistical information. We examine their ability to show areas of elevated WSS. We then evaluate whether the limitation to a static peak-systolic visualization leads to equal conclusions compared to the animated visualization, where the whole cardiac cycle is depicted. We also compare the results with the new statistical visualization and identify it as best suited for time-dependent WSS evaluation regarding depiction time and accuracy.

2 Materials and Methods

2.1 Medical Image Data and WSS Extraction

Our methods were applied to three aneurysm surface models extracted from three contrast-enhanced CT data sets DS_1, DS_2 and DS_3, see Fig. 1. For each of the image data sets, a 3D triangulated surface mesh was generated, which is described in more detail in our previous work [5]. Next, an unstructured volumetric grid with tetrahedral and prismatic elements was extracted from this surface mesh. It was employed as input for an unsteady hemodynamic CFD simulation using the finite volume solver ANSYS Fluent 14.0 (Ansys Inc., Canonsburg, PA, USA) yielding 4D vector fields approximating the internal blood flow. The WSS was extracted as: $\boldsymbol{\tau}_w = \eta \left(\frac{\partial \boldsymbol{v}}{\partial \hat{n}}\right)$, where η is the dynamic viscosity, $\boldsymbol{v}$ the velocity of flow and $\hat{n}$ the normalized surface normal of the surface mesh. Hence, we always employ the magnitude of the WSS.

2.2 Medical Image Visualization

For the WSS visualization, we developed three visualizations (recall Fig. 1):

- Vis_{PS} visualizes the WSS at peak systole,
- Vis_{SD} visualizes the WSS expectation value (μ) and standard deviation (σ),

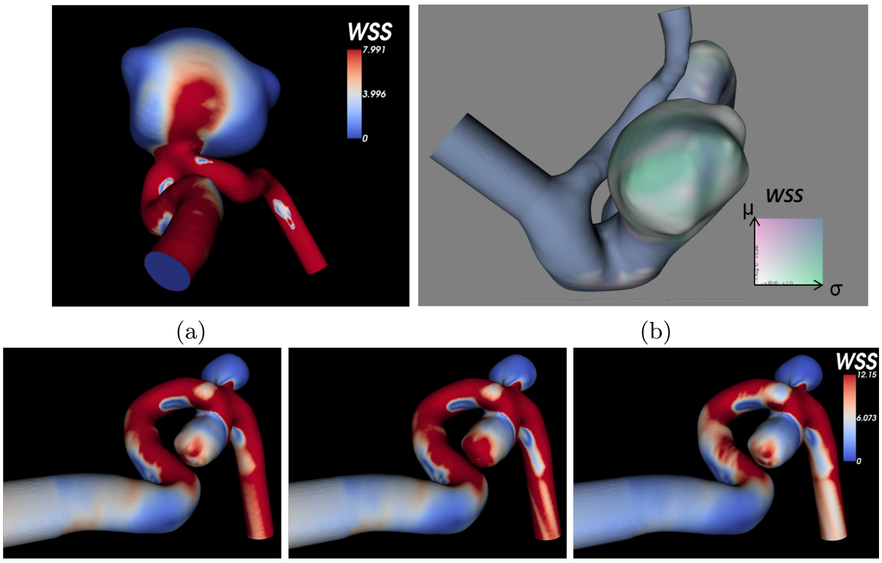

(a) (b)

(c)

Fig. 1. Depiction of the three data sets DS_1 (a), DS_2 (b), and DS_3 (c) as well as the visualization techniques Vis_{PS} (a), Vis_{SD} (b), and Vis_{Ani} (c).

– and Vis_{Ani} shows an animation of the WSS values.

The Vis_{PS} comprises a 3D surface representation with color-coded WSS. We employed a divergent color map, see Fig. 2. This color map is mostly used when a critical mid point exists, e.g., the freezing point of water. Although the WSS range lacks a critical mid point, the extrema of very high and very low WSS values exist. They can be easily recognized with this color map. Our color map is based on the color map in [6], which allows for the mapping of ordered values, accounts for red-green deficiency as well as brightness variations. This is important due to varying lighting or shading, which is required to present the geometrical shape of the aneurysm. The extrema red and blue yield three areas: very low WSS values (bluish colors), neutral WSS values (whitish colors) and elevated WSS values (reddish colors). Perceptually adapted brightness modification of the employed colors is realized with a transformation in the CIELAB color space with subsequent brightening.

For Vis_{SD}, a bivariate color map was employed, see Fig. 2. It was motivated by uncertainty visualizations, where temporal or statistical variations of parameters are mapped to static color representations [7]. Hence, variables with low variances were emphasized. In contrast, we are interested in the complete WSS range, including elevated and time-dependent WSS values with increased variances. Therefore, we developed a bivariate color map inspired by [8]. The influence of a single variable can be extracted based on the color hue and no ordering of the colors exists. For each vertex of the aneurysm surface mesh, μ

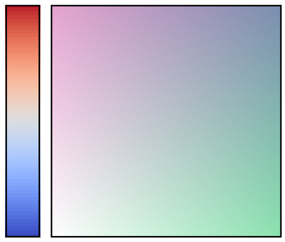

Fig. 2. Illustration of the employed color maps. On the left, the color map for the visualization techniques Vis_{PS} and Vis_{Ani} is depicted. On the right, the bivariate color map for Vis_{SD} is presented.

and σ were calculated for the whole cardiac cycle and the corresponding color was determined by linear interpolation. Thus, four extrema can be differentiated: white (low μ and low σ), pink (high μ and low σ), green (low μ and high σ), and blue (high μ and high σ).

The visualization technique Vis_{Ani} presents the animated WSS values of the cardiac cycle in a loop. The same color map as for Vis_{PS} is employed. The user can steer the animation by pressing "R" to restart with the first time step and the space key to pause it. Peak systole usually occurred during the first third of the cycle. Hence, the strongest WSS variations and highest WSS values could be observed. Pausing of the animation also supports the positioning of landmarks for the evaluation, which will be described in the next section.

Our visualization techniques were embedded in our prototype, developed with C++ and the VTK library (http://www.vtk.org). For the evaluation of the visualization techniques, we adapted our prototype and carried out a user study.

2.3 Evaluation with a User Study

We designed a single factor and between-subject study. The independent variable is the visualization technique which has three levels: Vis_{PS}, Vis_{SD} and Vis_{Ani}. The dependent variables comprise the precision of the placement and the number of landmarks. The landmarks were placed such that they mask the center of a hot spot. Hot spots are areas of the aneurysm surface with elevated WSS values with respect to their local neighborhood. From the medical point of view, parts of the aneurysm wall with low or oscillating WSS values may increase the rupture risk as well. However, we focused on elevated WSS values and their deviations to reduce the time consumption and the complexity of the user study. For the study, each participant processed the data sets DS_1 - DS_3. The visualization order was determined a priori with pseudo-randomization. 6 users (4 male, 2 female, age: 25 - 31 years) familiar with computer science, medicine and visualization participated. A ground truth was extracted by a neuroradiologist (more than 20 years of professional experience), who analyzed each data set with Vis_{Ani} and masked all hot spots with landmarks. For the distance extraction, the VTK-based technique determines the path (i.e., the shortest path between two vertices along the edges of the mesh) along the aneurysm surface. Although this may differ from the geodesic distance, the extracted values are sufficient to compare the different visualization techniques, since relative assumptions can be made.

	Vis_{PS}	Vis_{SD}	Vis_{Ani}
Minimum distance $[cm]$	0.055	0.037	0.014
Mean distance $[cm]$	0.34	0.18	0.13
Maximum distance $[cm]$	0.92	0.61	0.3

Table 1. Minimum, mean and maximum distances of the users' landmarks and the ground truth, averaged for each visualization technique.

		Vis_{PS}	Vis_{SD}	Vis_{Ani}	Ground Truth
μ (σ) of hot spots	DS_1	2.5 (0.71)	2.5 (2.12)	5 (2.83)	1
	DS_2	3.5 (2.12)	4.5 (0.71)	10 (2.83)	3
	DS_3	2 (0)	3.5 (0.71)	6.5 (0.71)	5
$\Delta DS_{1..3}$		1.67	1.5	4.17	–
t_{Eval} $[min]$		3.8	5.1	17.4	3.5

Table 2. Expected value (μ) and standard deviation (σ) for the number of landmarks for each data set and visualization as well as the required evaluation time t_{Eval} (averaged for all data sets). The values for $\Delta DS_{1..3}$ denote the averaged differences of the number of hot spots compared to the ground truth for Vis_{PS}, Vis_{SD}, and Vis_{Ani}.

3 Results

For the evaluation of our user study, we analyzed the users' landmarks determining their amount and positions as well as their distances to the nearest ground truth landmark. To get rid of distance measurement outliers, we remove user landmarks which do not correspond to any ground truth landmark, i.e., landmarks that exhibit a distance to the nearest ground truth landmark that exceeds an adjustable threshold. The results of our user study are listed in Tab. 2 and Tab. 1. As a result, the number of hot spots found as well as the time required for carrying out the evaluation are increasing with increasing complexity of the visualization technique, where Vis_{Ani} is more complex than Vis_{SD} and Vis_{SD} is more complex than Vis_{PS}. Furthermore, the number of hot spots found depends on the chosen visualization technique. Compared with the ground truth, the technique Vis_{SD} exhibits the smallest differences, recall Tab. 2. The distances between the users' landmarks and the ground truth are listed in Tab. 1. The average values for the minimum distance, the mean distance, and the maximum distance decreased for decreased complexity of the visualization. The least amount of outliers, i.e., the amount of selected hot spots that were not selected by the clinical expert, yielded Vis_{SD}. Although Vis_{Ani} exhibited slightly lower distances than Vis_{SD}, the latter is superior due to the amount of outliers. Most outliers occurred at the aneurysm neck, probably inflicted by the color map or the complex geometry.

4 Discussion

For the evaluation of time-dependent WSS, the visualization plays a critical role. As it was shown with the user study, the visualizations of unsteady CFD simulations, i.e., Vis_{Ani} and Vis_{SD}, reveal more and varying spatial areas with evaluated WSS values than the Vis_{PS}, i.e., the visualization of peak-systolic WSS. Therefore, we strongly recommend to employ Vis_{SD} or Vis_{Ani} for the detection of elevated time-dependent WSS and reject a restriction to peak-systolic WSS. When compared to the results of a clinical expert, our novel technique Vis_{SD} including statistical information achieved the closest match. Hence, Vis_{SD} is less time-consuming which may be a further advantage for clinical usability. The presented evaluation method includes the distance extraction between landmarks, which is sufficient for a qualitative comparison. For future work, a more precise distance extraction based on the geodesic distance could be approximated, as described in [9]. Furthermore, Vis_{Ani} could be improved w.r.t. the users' suggestions. They demanded further control for replaying the animation as well as an illustration of the cardiac cycle. Thus, they could focus on the most interesting point in time and probably evaluate the animated WSS in a faster way.

Acknowledgements This work was partly funded by the German Federal Ministry of Education and Research within the Forschungscampus STIMULATE (grant number: 13GW0095A).

References

1. Cebral JR, Castro M, Appanaboyina S, Putman CM, Millan D, Frangi AF. Efficient Pipeline for Image-Based Patient-Specific Analysis of Cerebral Aneurysm Hemodynamics: Technique and Sensitivity. IEEE Trans Med Imaging. 2005;24(4):457–467.
2. Papaioannou TG, Stefanadasi C. Vascular Wall Shear Stress: Basic Principles and Methods. Hellenic Journal Cardiology. 2005;46(1):9–15.
3. Jhunjhunwala P, Padole P, Thombre S. CFD Analysis of Pulsatile Flow and Non-Newtonian Behavior of Blood in Arteries. MCB: Molecular & Cellular Biomechanics. 2015;12(1):37–47.
4. Geers AJ, Larrabide I, Morales HG, Frangi AF. Approximating Hemodynamics of Cerebral Aneurysms With Steady Flow Simulations. Journal of Biomechanics. 2014;47(1):178–185.
5. Glaßer S, Berg P, Neugebauer M, Preim B. Reconstruction of 3D Surface Meshes for Bood Flow Simulations of Intracranial Aneurysms. In: Proc. of Tagung für Computer- und Roboterassistierte Chirurgie (CURAC); 2015. p. 163–168.
6. Moreland K. Diverging Color Maps for Scientific Visualization. In: Proc. of the Int. Symposium on Advances in Visual Computing: Part II; 2009. p. 92–103.
7. Potter K, Kirby M, Xiu D, Johnson CR. Interactive Visualization of Probability and Cumulative Density Functions. International Journal for Uncertainty Quantification. 2012;2(4):397–412.
8. Stevens J. Bivariate Choropleth Maps: A How-to Guide; 2015. Available from: http://www.joshuastevens.net/cartography/make-a-bivariate-choropleth-map.
9. Polthier K, Schmies M. Straightest Geodesics on Polyhedral Surfaces. In: ACM SIGGRAPH 2006 Courses; 2006. p. 30–38.